

# MUON COLLIDER FINAL COOLING IN 30-50 T SOLENOIDS\*

Robert B. Palmer, Richard C. Fernow, BNL, Upton, New York, USA  
 Jon Lederman, UCLA, Los Angeles, California, USA

## Abstract

Muon ionization cooling to the required normalized rms emittance of 25 microns transverse, and 72 mm longitudinal, can be achieved with liquid hydrogen in high field solenoids, provided that the momenta are low enough. At low momenta, the longitudinal emittance rises from the negative slope of energy loss versus energy. Assuming initial emittances that have been achieved in six dimensional cooling simulations, optimized designs are given using solenoid fields limited to 30, 40, and 50 T. The required final emittances are achieved for the two higher field cases.

## INTRODUCTION

A multi-TeV muon collider would be smaller, use less power, and hopefully be cheaper than an  $e^+ - e^-$  collider with the same performance, but there are significant challenges. Muons are made by pion decay with large emittances. These emittances must be reduced (cooled) in all 6 dimensions.

Reduction of transverse phase space is achieved by ionization cooling[1]. Reduction of longitudinal phase space is achieved using a combination of more transverse cooling, together with emittance exchange. Several schemes have been studied, and two of them [2, 3] appear capable of reducing the emittances to 400  $\mu\text{m}$  transverse, and 1 mm longitudinal (all emittances quoted are rms & normalized). A 1.5 TeV (c-of-m) collider ring has been designed[4] that achieves a luminosity of  $1 \times 10^{34} \text{ cm}^{-2} \text{ sec}^{-1}$ , using transverse emittances of 25  $\mu\text{m}$ . This is much less than what is achieved in these 6D cooling schemes. On the other hand the ring can accept a longitudinal emittance of 72 mm, which is much larger than that from the 6D cooling. This allows a complete scheme [5] with final cooling that acts only in the transverse dimensions, while allowing the longitudinal to grow.

The minimum transverse emittances achievable in hydrogen in a long solenoid field  $B$  is given by:

$$\epsilon_{x,y}(\text{min}) \propto \frac{E}{B L_R dE/dz}$$

where  $L_R$  is the material radiation length,  $dE/dz$  is the energy loss per unit length, and  $E$  is the muon energy. Values of  $\epsilon_{x,y}$  for 3 solenoid fields are plotted against energy in Fig.1a. As the muon energy  $E$  falls, aided by the increase in  $dE/dz$ , the minimum emittance can reach below 25  $\mu\text{m}$  at low enough energies. At these energies, the energy loss (Fig.1b) has a strong negative slope that increases momentum spread, and thus longitudinal emittance. But providing

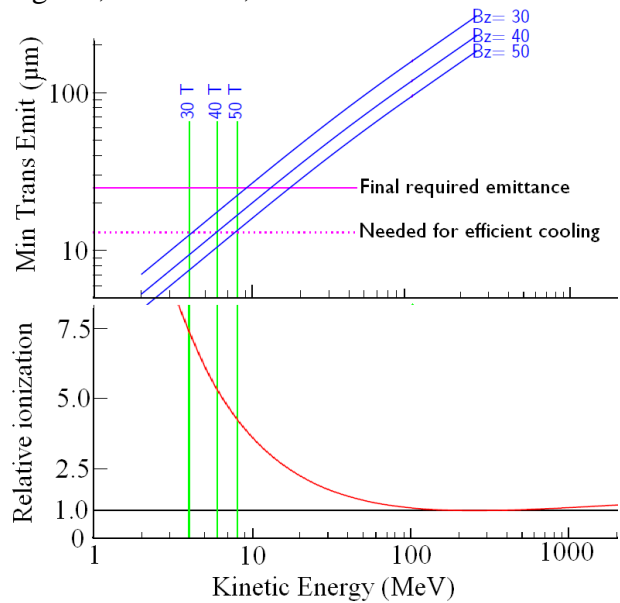


Figure 1: a) Minimum transverse emittances vs. muon energy for three magnetic fields; b) energy loss vs. energy.

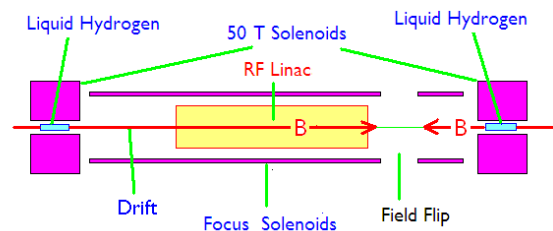


Figure 2: Schematic of one stage of final cooling.

this slope  $-d\epsilon_{\parallel}/d\epsilon_{\perp}$  is not too great, the required transverse emittance can be reached with acceptable longitudinal emittance.

## FINAL COOLING SEQUENCES

The proposed final cooling system consists of a dozen or so stages. Each stage consists (see Fig. 2) of a high field, small bore solenoid, inside which the muons pass through a liquid hydrogen absorber. Between each solenoid there is rf to re-accelerate and phase-rotate the muons, giving the required energy and energy spread for the following stage. There is also a field reversal to avoid an accumulation of canonical angular momentum. Fig. 3 shows a 40 T example of an ICOOL[6] simulation of the falling energy and transverse emittance, and rising longitudinal emittance.

\* Work supported by US Department of Energy under contract DE-AC02-98CH10886 and DE-FG02-08ER85037

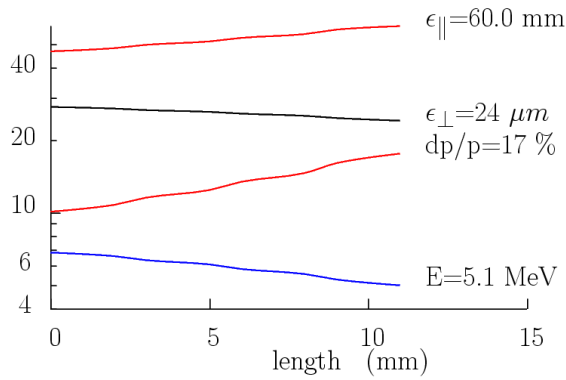


Figure 3: Parameters vs. length for ICOOL simulation of cooling in one 40 T solenoid.

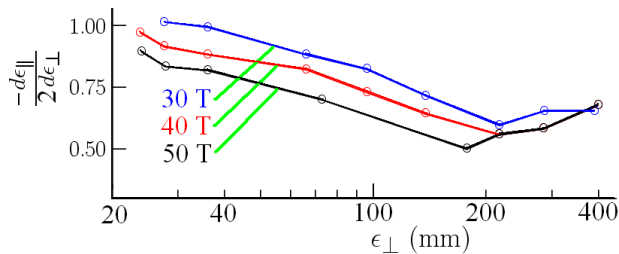


Figure 4: One half the ratio of longitudinal to transverse emittance changes vs. representative initial transverse emittances. Values  $< 1.0$  give finite 6D cooling;  $1.0$  gives constant 6D emittance.

### Optimized Stages

For each stage, the initial energy, energy spread, and absorber length, can be adjusted to minimize the ICOOL simulated negative slope  $-d\epsilon_{\parallel}/d\epsilon_{\perp}$ . Fig. 4 shows negative slopes for manually optimized stages, starting from several representative initial emittances. These were obtained using three different solenoid fields: 30, 40, and 50 T.

Assuming that we can use linear interpolation of the slopes, and other parameters, at intermediate initial emittances, we obtain longitudinal vs. transverse emittances for full sequences using the three fields (see Fig. 5). The sequences start from a transverse emittance of  $400 \mu\text{m}$ , and longitudinal emittance of  $1 \text{ mm}$ , as achieved at the end of the earlier systems of 6D cooling.

From Fig. 4, we note that, starting from the right ( $\epsilon_{\perp} = 400 \mu\text{m}$ ), the negative slopes initially fall, i.e. the cooling improves. Here, the bunch length must be kept up to avoid emittance growth from amplitude dependent transit times. With the longitudinal emittance still small, one must use non-optimally small initial momentum spreads  $dp/p$ , and low initial energies (67 MeV). As the longitudinal emittance rises, more optimum momentum spreads and initial energies can be used, the cooling becomes more efficient, and the negative slopes fall. In this regime, the advantages of raising the magnetic field are largely cancelled by the worse transit time variations that they produce.

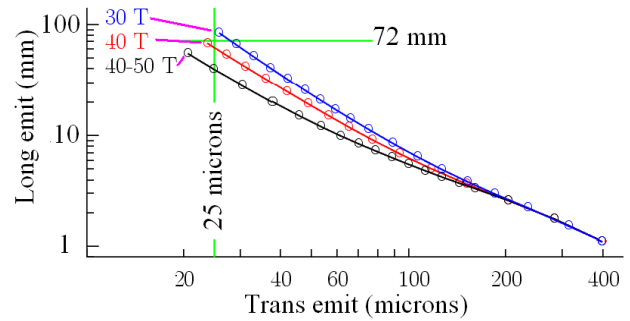


Figure 5: Longitudinal vs. transverse emittances for sequences of stages using three solenoid fields.

Later ( $\epsilon_{\perp} < 200 \mu\text{m}$ ), when the increased longitudinal emittances allow sufficient bunch length with optimized momentum spreads, getting a low enough equilibrium transverse emittance becomes the dominant problem. For this, the energy must be further lowered, increasing the growth of longitudinal emittance, giving less efficient cooling, and thus rising negative slopes. Now, a higher magnetic field, by reducing the need for lower energies, increases the efficiency, and gives lower negative slopes.

From Fig. 5, we note that the 50 T case more than achieves our requirements, while 40 T just meets them. 30 T just misses the requirement, but could probably be acceptable with some adjustment of parameters.

### 40 T Example

Fig. 6 shows some parameters vs. stage for the 40 T case. The energy falls in steps from 66 MeV to its final value of 5.1 MeV, while the bunch length rises from 5 to 400 cm. The lengths of hydrogen absorber fall from 77 cm to 1.1 cm, as the energy falls and  $dE/dz$  increases. The final beam  $\beta$  is 1.5 cm, giving an rms beam size of 0.6 mm.

Table 1 shows the assumed parameters for the rf. For bunches shorter than 0.75 m, the rf frequencies were chosen to keep  $\sigma_{ct} < \lambda/20$ . The gradients assumed maximum surface fields  $\propto \sqrt{f}$ , and, assuming reentrant vacuum cavities with surface to accelerating gradients  $\propto f^{0.75}$ . For bunches longer than 0.75 m, induction linacs with gradients of 1 MV/m were assumed.

Fig. 7 shows the lengths of the different elements in this example. These are obtained by adding magnet lengths to calculated lengths for phase rotation and re-acceleration. When correctly simulated, the lengths should be shorter because some rotation will occur in the magnet ends, and during acceleration.

The simulated loss, excluding decay, but including 3 sigma cuts, is 17.7%. The calculated decay loss is 19%, giving a total transmission of 67%.

### Matching and Re-acceleration

The matching, re-acceleration and field flips have been fully simulated for only one case: that between the last

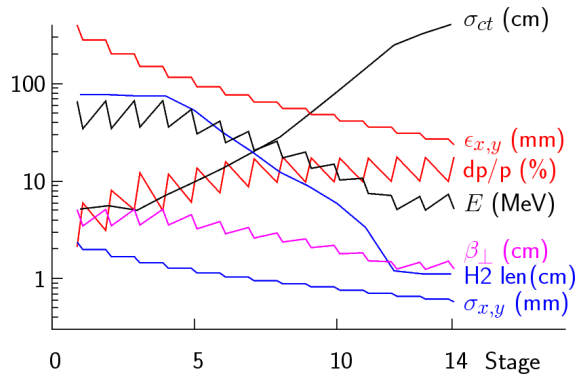


Figure 6: Some parameters vs. stage for the 40 T sequence.

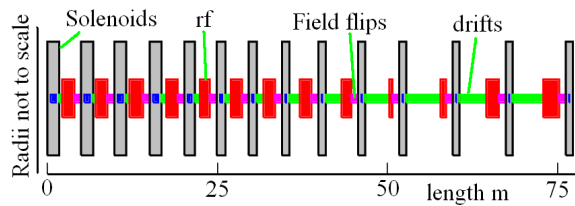


Figure 7: Lengths of elements in the optimized sequence using 40 T solenoids.

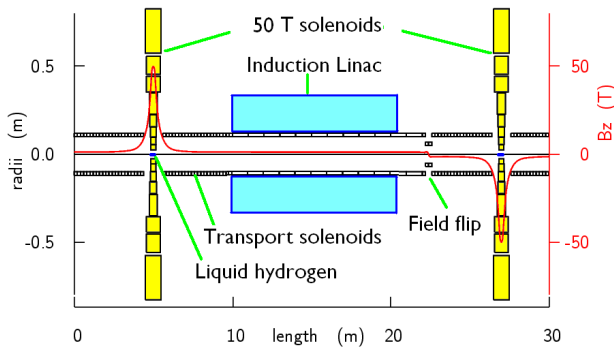


Figure 8: Design of matching and acceleration for the last two stages of the 50 T sequence.

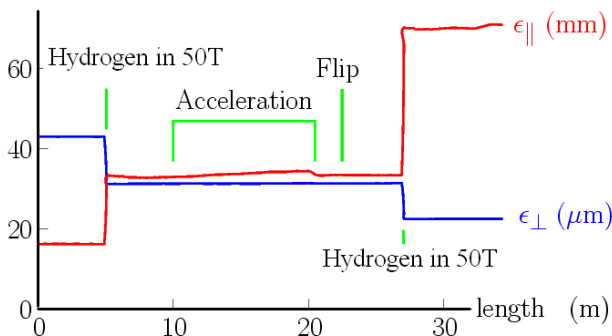


Figure 9: Simulation of matching and acceleration for the last two stages of the 50 T sequence.

Table 1: Rf Parameters of 40 T Example

	E1 MeV	E2 MeV	freq MHz	grad MV/m	acc L m
NCRF	34.6	66.6	201	15.5	2.1
NCRF	34.8	66.9	201	15.5	2.1
NCRF	36.0	67.1	201	15.5	2.0
NCRF	36.0	54.5	153	11.1	1.7
NCRF	30.6	41.3	110	7.4	1.5
NCRF	24.9	32.4	77	4.7	1.6
NCRF	20.7	25.7	53	2.9	1.7
NCRF	17.4	20.0	31	1.5	1.7
Induction	13.6	15.0	18	1.0	1.4
Induction	10.3	10.7	10	1.0	0.4
Induction	7.5	7.2	6	1.0	0.7
Induction	5.1	7.0	5	1.0	1.8
Induction	5.1	7.4	4	1.0	2.3

two stages of the 50 T example. Fig. 8 shows a highly compressed representation of its elements. In this case, the bunch is very long ( $\approx 3$  m), and the rf is an induction linac. Fig. 9 shows the simulated longitudinal and transverse emittances vs. the length. In this example, the simulated emittance dilutions in the acceleration are acceptable: 0.1% transversely and 0.5% longitudinally. The simulated losses are 7.3%, significantly less than the value of 10% estimated from the above assumptions. This is encouraging, but similar simulations of matching and re-acceleration for earlier stages are essential.

### CONCLUSION & PROSPECTS

Preliminary simulations of transverse cooling in hydrogen, at low energies, suggests that muon collider emittance requirements can be met using solenoid fields of 40 T or more. It might also be acceptable with 30 T. But these simulations did not include hydrogen windows, matching or re-acceleration, whose performance, with one exception, was based on numerical estimates. Full simulations of more stages are planned. The design and simulation of hydrogen windows must be included, and space charge effects, and absorber heating, calculated.

### REFERENCES

- [1] G. I. Budker, 1969 Yerevan Conference, AIP Conf. Proc.352 (1996) 4; G. I. Budker, 1970 Kiev Conference, AIP Conf. Proc.352 (1996) 5
- [2] R.B. Palmer et al., Phys. Rev. Spec. Top. - Acc. & Beams 8, 061003 (2005).
- [3] Y. Derbenev and R. P. Johnson, Phys. Rev. Spec. Top. - Acc. & Beams 8, 041002 (2005).
- [4] Y. Alexahin et al., Proc. 2010 IPAC Conf., p. 1563.
- [5] R.B. Palmer et al., A Complete Scheme of Ionization Cooling for a Muon Collider, PAC07 (2007), p. 3193.
- [6] R. Fernow, Proc. 2005 Part. Acc. Conf., p. 2651.